Available online at www.sciencedirect.com
ScienceDirect
Advances in Space Research 44 (2009) 451–456
ADVANCES IN SPACE RESEARCH (a COSPAR publication)
www.elsevier.com/locate/asr

Interpretation of the SOHO/UVCS observations of two CME-driven shocks

Salvatore Mancuso, Alessandro Bemporad *

Istituto Nazionale di Astrofisica (INAF), Osservatorio Astronomico di Torino, Strada Osservatorio 20, 10025 Pino Torinese, Torino, Italy

Received 27 January 2009; received in revised form 20 March 2009; accepted 25 March 2009

Abstract

We report on the analysis of two fast CME-driven shocks observed with the UltraViolet Coronagraph Spectrometer (UVCS) on board the Solar and Heliospheric Observatory (SOHO). The first event, detected on 2002 March 22 at 4.1 $R_\odot$ with the UVCS slit placed in correspondence with the flank of the expanding CME surface, represents the highest UV detection of a shock obtained so far with the UVCS instrument in the corona. The second one, detected on 2002 July 23 at 1.6 $R_\odot$ with the UVCS slit placed in correspondence with the front of the expanding CME surface, shows an anomalous deficiency of ion heating with respect to what observed in previous CME/shocks observed by UVCS, possibly reflecting the effect of different coronal plasma conditions over the solar cycle. From the two different sets of observations we derived an estimate for the shock compression ratio X, which turns out to be $X = 2.4 \pm 0.2$ and $X = 2.2 \pm 0.1$, respectively, for the first and second event. Comparison between the two events provides complementary perspectives on the dynamical evolution of CME-driven shocks.

Keywords: Sun: coronal mass ejections (CME); Sun: UV radiation; Shock waves

1. Introduction

Coronal shock observations can be used as unique diagnostic tools for estimating important physical properties (electron density, magnetic field, plasma β, etc.) of the solar corona. CME-driven shocks are caused by the difference in speed between the faster CME and the slower solar wind. When this difference is larger than the local solar wind magnetosonic speed, a fast-mode MHD shock forms ahead of the CME. In general, frequency-drifting radio bursts, which appear as narrow bands of enhanced emission in metric-range dynamic spectra, are the clearest signature of shock waves travelling through the solar corona. These so-called type II radio bursts are attributed to accelerated beams of electrons exciting plasma waves that in turn non-linearly convert into escaping electromagnetic waves. The observed emission at the plasma frequency relates directly to the local electron density $\left(f \simeq f_{pe} = \sqrt{\frac{e^2 n_e}{m_e \pi}} \propto \sqrt{n_e}\right)$, and thus to the burst driver's height under the assumption of a coronal density model. Although type II signatures are detected by ground and space radio spectrometers on a daily basis, direct imaging of coronal shocks remains an outstanding observational challenge. Radioheliograph observations of type II radio bursts are rare and known to be affected by propagation effects, such as refraction and ducting, while shock identification with observed features in coronagraphic white-light images (e.g. Vourlidas et al., 2003, 2006) is problematic, due to the uncertainty in differentiating between hot, shock-compressed plasma, and ejected prominence material. Very recently, Ontiveros and Vourlidas (2009) demonstrated that for stronger events ($v > 1500$ km s^{-1}) the CME-driven shock is indeed visible in coronagraphic images and that the shock strength can be estimated. However, coronagraphic images are able to provide informations only on the density variations related

* Corresponding author. Tel.: +39 011 8101 954; fax: +39 011 8101 930.
E-mail addresses: mancuso@oato.inaf.it (S. Mancuso), bemporad@oato.inaf.it (A. Bemporad).

0273-1177/$36.00 © 2009 COSPAR. Published by Elsevier Ltd. All rights reserved.
doi:10.1016/j.asr.2009.03.021

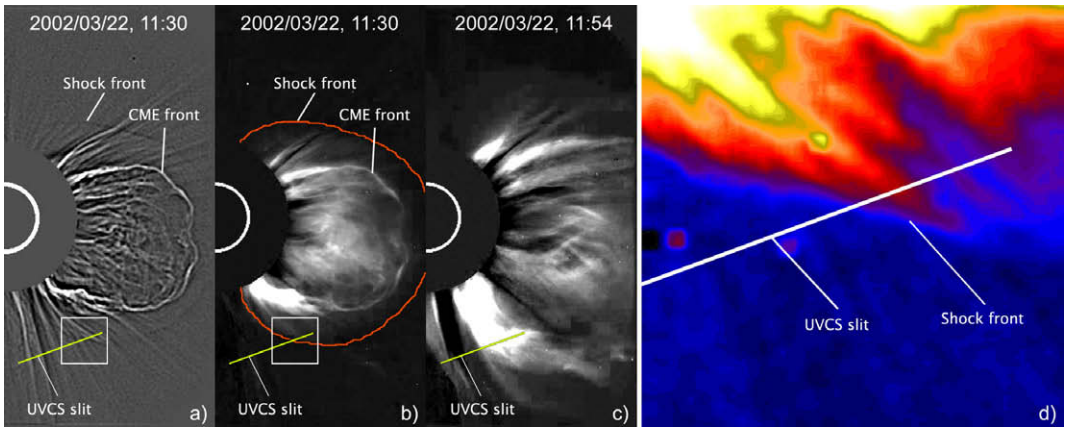

Fig. 1. LASCO/C2 wavelet (a) and base difference (b) images showing the white light corona during the transit of the CME-driven shock front through the UVCS slit at 11:30 UT, and a base difference image 24 min later (c). The solid line in (b) underlines the position of the shock front visible in the wavelet image (a). (d) shows a zoom on the coronal region where the shock front crosses the UVCS slit (white boxes in (a) and (b)).

to the shock transit; in order to measure other plasma physical parameters it is necessary to use spectroscopic data. In the last decade ultraviolet spectroscopy, combined with other remote-sensing observations, has allowed the breakthrough detection of shock formation in the corona (e.g. Raymond et al., 2000; Mancuso et al., 2002) with the Ultraviolet Coronagraph Spectrometer (UVCS; Kohl et al., 1995) on board the Solar and Heliospheric Observatory (SOHO). CME-driven shocks in the ultraviolet have been identified as wide and sudden broadenings of the O VI spectral line profiles, together with simultaneous brightenings of spectral lines from heavier ions. In the present work, we analyze the evolution of two CME/shock events observed by UVCS. In particular, we will obtain estimates of the compression ratios for both events and we will discuss how such a knowledge can be used to extract information on the coronal plasma properties in the region of propagation of the shock (Alfvénic Mach number, magnetic field strength, etc.).

2. CME-driven shock events

2.1. 2002 March 22 event

The fast halo-CME event of 2002 March 22 was associated with a M1.6 flare originating from the active region NOAA AR 9866, located near the west limb. An intense solar proton event (SPE) and a strong, complex metric/decametric type II radio burst were also associated to this event. According to the measurements compiled in the online LASCO CME Catalog[1] (Gopalswamy et al., 2009), the CME leading edge was first detected in white-light by the Large Angle Spectrometric Coronagraph (Brueckner et al., 1995, LASCO;) aboard SOHO at a projected height of 3.1 $R_\odot$ starting from 11:06 UT and expanding westward with a speed of 1750 km s^{-1}. The extrapolated CME onset was estimated around 10:52 UT, well after the flare onset (10:12 UT) but still during its rising phase (the flare's peak occurred at 11:14 UT). Fig. 1 shows the LASCO/C2 wavelet enhanced (panel a) and base difference (panel b) images taken during the passage of the shock front through the UVCS slit and the successive base difference image (panel c).

At the time of the CME passage, UVCS was observing above the southwest limb with its entrance slit centered at a latitude of 70° SW and a height of 4.1 $R_\odot$ from the center of the Sun. UVCS is a long-slit UV spectrograph for the observation of spectral lines in the extended solar corona with an instantaneous field of view of 42′ tangent to the limb of the Sun. The UVCS telescope mirror and instrument rotation mechanisms can point the spectrograph slit along the radial direction to observe the entire corona at heliocentric distances between 1.5 and 10 $R_\odot$. A complete description of the UVCS instrument is provided in Kohl et al. (1995). The entire set of observations comprised 171 exposures of 200 s each, starting from 08:20 to 18:29 UT, encompassing the whole CME/shock event. The most prominent spectral lines detected during the CME passage through the UVCS slit (panel d in Fig. 1) were the O VI $\lambda\lambda$ 1031.9, 1037.6 doublet and the H I Lyα 1215.67 Å lines. The left panel of Fig. 2 shows the spatio-temporal evolution of the Lyα line intensity during the transit of the shock front (dashed line) through the UVCS slit. On the right panel, we also show the time evolution of the O VI and Lyα intensities averaged over an angular interval of ~6° at the eastward edge of the slit during the passage of the shock front through the UVCS slit. At the shock passage, the Lyα intensity was severely dimmed, because the coronal plasma in the region crossed by the CME is accelerated by the shock wave up to $v_{shock} \times (1 - 1/X) \sim 1000$ km s^{-1} (with $v_{shock} \sim 1700$ km s^{-1} estimated from LASCO images). Since this line is almost entirely radiatively excited, it is completely Doppler

[1] See http://cdaw.gsfc.nasa.gov/CME_list/

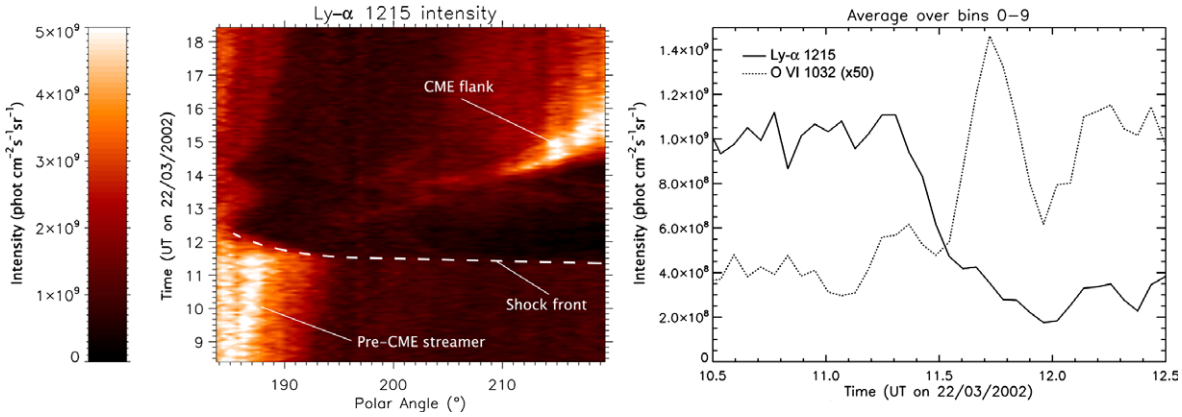

Fig. 2. Left: space–time dependence of the Lyα line intensity observed during the passage of the shock front (dashed line) through the UVCS slit. The position along the slit of a pre-CME streamer (not visible in the LASCO base difference images) is also shown. Right: the time evolution of the O VI λ1032 (dotted line) and Lyα λ1216 (solid line) intensities averaged over an angular interval of ~6° (10 spatial bins) at the eastward edge of the slit.

dimmed. On the contrary, the O VI line intensities were suddenly enhanced a few exposures later due to a combination of plasma compression of the shocked plasma and possible contribution from hot CME material (see later on). Unfortunately, because of the low count rate, it was not possible to observe the expected broadening of the shocked O VI line profiles (e.g. Mancuso et al., 2002; Pagano et al., 2008). A simultaneous metric type II radio burst was reported in the Solar Geophysical Data (SGD) by the Izmiran (Russia) radio observatory starting at 11:08.4 UT at a frequency of 70 MHz and ending at 11:10.6 UT at 55 MHz. Although not reported in the SGD, the same event was also detected by the Astrophysical Institute Potsdam (Germany) radio-spectrometer as a complex, low-frequency type II radio burst feature starting around 11:08 UT and lasting about ten minutes (H. Aurass 2008, private communication). The analysis of the radio data, which will allow for an estimate of the shock dynamics, is presently ongoing. A strong type II feature associated with the same event, was finally observed by the Radio and Plasma Waves (WAVES) experiment on board the Wind spacecraft (Bougeret et al., 1995) as a bright, multi-component emission, indicating that the shock was further piston-driven outward in the solar wind.

The LASCO/C2 base difference images (obtained by subtracting from all images the last one before the CME occurrence) can be used to distinguish between the shock-compressed plasma and the CME material. In particular, a wavelet image taken from the online LASCO wavelet catalog[2] at 11:30 UT shows the presence of an enhanced arch-shaped density region preceding the expanding CME front (Fig. 1, panel a). In general, the wavelet transform is able to discriminate structures as a function of scale, and can help the identification of smaller scale structures, such as thin discontinuity surfaces, embedded within larger scale features. In this work, we interpreted this enhanced density, outlined by a solid line in Fig. 1 (panel b), as the downstream plasma compressed by the shock transit. Adopting this interpretation, LASCO/C2 images can be used to infer the compression ratio X between the downstream n_d and upstream n_d plasma densities $X = n_d/n_u$. Since the white-light brightness observed in LASCO images results from the integration along the line of sight (LOS) of disk-emitted Thomson-scattered photons, in order to estimate X we need to assume both a density profile $n_e(r)$ and a shock depth L along the LOS. Given the density profile, the expected white light total brightness $B/B_\odot(\rho)$ at a projected altitude ρ can be computed from an integration along the line of sight (see Van de Hulst, 1950). From the observed jump in the white light intensity across the shock, by assuming the shock depth L along the line of sight, it is possible to estimate the relative electron density increase with respect to the pre-shocked corona, hence the compression ratio X.

Many coronal density radial profiles, derived from UV or white light observations, are available in the literature. In this work, we used the coronal streamer profile from Gibson et al. (1999) and the coronal hole density profile from Cranmer et al. (1999), respectively. The shock depth L is a crucial parameter, because the derived X value decrease for larger L values and vice-versa; however, the real three-dimensional geometry of the shock is at present unknown. In this work we assume that the shock depth L is of the same order than the observed thickness projected on the plane of the sky, $L = (5 \pm 1) \times 10^4$ km; this is only a lower limit estimate to the actual L value, hence the derived compression ratio X will have to be considered as an upper limit estimate. With this depth L we obtain a compression ratio $X \leqslant 2.2 \pm 0.1$ with the Gibson et al. (1999) profile and a slightly larger value, $X \leqslant 2.6 \pm 0.2$, with the Cranmer et al. (1999) profile. On average, from the LASCO/C2 images, we thus estimate a compression ratio $X \leqslant 2.4 \pm 0.2$. The above empirical value is an important input parameter in order to characterize the shock and the physical properties of the plasma through which it

[2] See http://lasco-www.nrl.navy.mil/wavelet/

propagates. In particular, it can be used to estimate the Alfvénic Mach number M_A of the upstream plasma, i.e. the ratio between the upstream velocity v_u (measured in a reference frame at rest with the shock front) and the local Alfvén velocity v_A (e.g. Mancuso et al., 2003). These latter are key parameters for the implementation of any CME model. Having obtained an estimate of the local coronal density, these parameters further allow for an estimate of the coronal magnetic field strength.

As shown in Fig. 2, during the CME transit across the UVCS slit, the EUV line intensities changed significantly. However, the observed line intensity variations were relatively small when compared to analogous CME/shock observations previously reported by UVCS studies, where increases in the EUV emission even by orders of magnitude have been detected. This is due to the fact that all previous CME/shock events were typically observed by UVCS below $\sim$2.5 $R_\odot$. The peculiarity of this event is that it has been observed at 4.1 $R_\odot$: as the CME expands both the electron density and – because of the adiabatic expansion – the electron temperature decrease, so that it is likely to expect a rapid decrease in the EUV emission from the CME. It is interesting to note the different behaviours of the Lyα and O VI line intensity temporal evolution shown in the right panel of Fig. 2: the Lyα intensity is completely smeared out by the transit of the shock (and, later on, of the CME) because of the mentioned Doppler dimming effect. On the contrary, the O VI line is due both to radiative and collisional excitations: at $v_{shock} \simeq 1000$ km s^{-1} the radiative component is completely Doppler dimmed, while the collisional component, being roughly proportional to n_e^2, is visible. The first peak, visible in the O VI line intensity evolution at about 11:20 UT, and centered around the time the Lyα intensity starts to decrease, can thus be interpreted as the shock signature, while the second peak, centered around 11:40 UT, can be ascribed to the arrival of the CME front.

2.2. 2002 July 23 event

On 2002 July 23, a very fast CME ($v \simeq 2300$ km s^{-1}) occurred above the East limb (Fig. 3). This event was associated with a strong X4.8 class flare from active region NOAA AR 0039 (beginning at 00:23 UT and reaching a peak at 00:29 UT). It was also accompanied by an intense and complex "band-splitted" type II radio emission. Band-splitting in type II bursts is usually ascribed to radio emission from the upstream and downstream plasma emitted at the respective frequencies f_u and f_d (e.g. Smerd et al., 1974; Vršnak et al., 2001). At the time of the CME passage, the UVCS slit was placed near the East limb at a mirror height of 1.63 $R_\odot$ from the center of the Sun, so that it was possible to observe the full evolution of the CME-driven shock as it crossed the spectrometer slit. Also in this case, as in the previous event, the EUV lines observed by UVCS changed noticeably during the shock transit across the slit: the Lyα line intensity decreased (because of the abrupt acceleration of the plasma and the subsequent reduction of the radiative component due to Doppler dimming), while the O VI spectral lines, whose profiles were well-defined because of the high count statistics, were broadened by a large factor (due to shock heating of heavy ions and bulk motion of the CME-expanding material along the line of sight). The analysis of UVCS data relative to this shock has been already discussed by Mancuso and Avetta (2008). The result of Mancuso and Avetta (2008) was suggestive of a different ion heating mechanism operating in the event of 2002 July 23 with respect to the ones acting on the plasma heated by previous CME/shock events examined by UVCS. In particular, it was suggested that the shock was propagating through a larger plasma β, a fact that is known to affect ion heating (e.g. Korreck et al., 2007). Also for this event, we are able to estimate the compression ratio. In fact, from the observed type II band-splitting ($f_d - f_u \approx 20$ MHz), and bearing in mind that the frequency f of the radio emission is close to the local electron plasma frequency, $f \simeq f_{pe} \propto \sqrt{n_e}$, it is possible to estimate $X = n_d/n_u = (f_d/f_u)^2$. The instantaneous compression ratio computed in this way is $X = 2.2 \pm 0.1$, implying a strong compression behind the shock front.

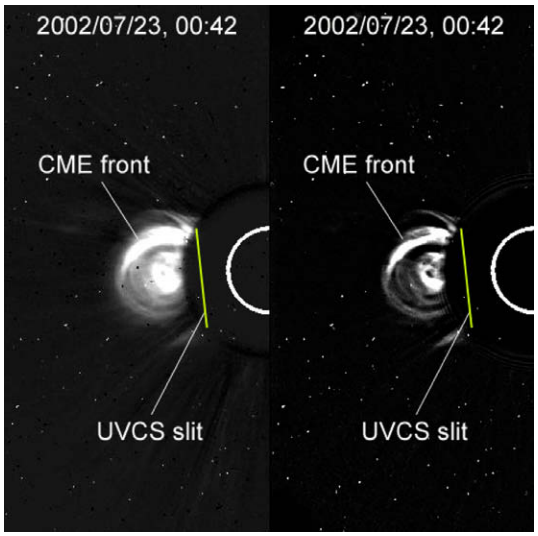

Fig. 3. Left: LASCO/C2 image obtained at 00:42 UT during the CME passage above the East limb on 2002 July 23; the solid line, perpendicular to the radial direction, shows the position of the UVCS slit field of view. This is the first LASCO/C2 frame where the CME was front visible, while in the following frame, acquired at 01:31 UT, the CME leading edge surface was already beyond the telescope field of view. Right: the same image, edge enhanced with wavelet transforms in order to better show the shape of the CME front.

3. Discussion and conclusions

In this work, we analyzed white light, radio, and EUV data related to two CME-driven shocks observed on 2002 March 22 and July 23. The CME fronts presented a clear shock signature both in EUV and white-light. For the first event, observed with the UVCS slit at 4.1 $R_\odot$, we estimated,

from white-light data, an upper limit estimate to the compression ratio $X \sim 2.4 \pm 0.2$, while, for the second event, observed at 1.6 $R_\odot$, we derived, from radio data, a compression ratio $X \sim 2.2 \pm 0.1$. These values, similar to X values recently measured by Ontiveros and Vourlidas (2009) from SOHO/LASCO data, can be used in order to estimate the local Alfvén Mach number: for example, in the case of a perpendicular shock, the Alfvénic Mach number M_A can be expressed as $M_A = \left[\frac{X(X+5+5\beta)}{2(4-X)}\right]^{1/2}$ (e.g. Vršnak et al., 2002), where $\beta = p_{gas}/p_{mag}$ is the ratio between the gas pressure, $p_{gas} = 2n_e k_B T$, and the magnetic pressure, $p_{mag} = B^2/8\pi$. For a longitudinal shock, more simply, $M_A = \sqrt{X}$. In the limiting case of $\beta \to 0$, the above formulas yield $\sqrt{X} \leqslant M_A \leqslant \sqrt{X(X+5)/[2(4-X)]}$, hence in particular $1.5 \lesssim M_A \lesssim 2.4$ for the 2002 March 22 event and $1.5 \lesssim M_A \lesssim 2.1$ for the 2002 July 23 event. These results can be compared with the previous estimates obtained by Smerd et al. (1974) and Vršnak et al. (2002) that found $1.2 \lesssim M_A \lesssim 1.7$ for perpendicular propagation.

The above expressions for M_A, given for the two extreme cases of longitudinal and perpendicular shocks, are, however, simplistic approximations derived from the more general Rankine–Hugoniot equations for oblique shocks (e.g. Priest, 1982). Actually, the LASCO/C2 images acquired on 2002 March 22 show that the CME-driven shock front, when crossing the UVCS slit, is inclined with respect to the radial direction by a large amount (see Fig. 1). By assuming that, at the altitude of 4.1 $R_\odot$, the magnetic field is nearly radial, this implies that the angle θ_{shock} between the normal to the shock front and the upstream magnetic field is neither near 0° nor near 90°. Similar considerations can be made for the flanks of the shock front surface intersecting the UVCS slit in the case of the second event considered in this work. As a consequence, in order to study these events and retrieve reliable information about the coronal plasma parameters, we need to apply the more general MHD Rankine–Hugoniot equations for oblique shocks. In particular, once the compression ratio X is known, given the geometry (θ_{shock}), and having obtained estimates for all the upstream plasma parameters (i.e., density, temperature, and velocity), which are assessable through the UVCS diagnostics (e.g. Bemporad et al., 2007), the MHD Rankine–Hugoniot equations can be used in order to derive both the up- and downstream magnetic field strengths. In fact, we are interested in the intrinsic potential of UVCS observations as a diagnostic tool for estimating the coronal magnetic field, a plasma parameter that is widely uncertain in the outer corona. Such knowledge, that is crucial for testing computational models of the solar corona, would be particularly important since there are very few estimates of the magnetic field above a few solar radii in the outer corona (e.g. Dulk et al., 1976; Patzold et al., 1987; Mancuso and Spangler, 2000; Ingleby et al., 2007).

Acknowledgments

The authors acknowledge the financial support from contract ASI–INAF I/015/07/0. The authors are also thankful to H. Aurass for providing and commenting the radio data from the Potsdam Observatory. SOHO is a project of international cooperation between ESA and NASA. The LASCO CME Catalog is generated and maintained by NASA and Catholic University of America in co-operation with the Naval Research laboratory.

References

Bemporad, A., Raymond, J., Poletto, G., Romoli, M. A Comprehensive Study of the Initiation and Early Evolution of a Coronal Mass Ejection from Ultraviolet and White-Light Data. Astrophys. J. 655, 576–590, 2007.

Bougeret, J.-L., Kaiser, M.L., Kellogg, P.J., et al. Waves: The Radio and Plasma Wave Investigation on the Wind Spacecraft. Space Sci. Rev. 71, 231–263, 1995.

Brueckner, G.E., Howard, R.A., Koomen, M.J., et al. The Large Angle Spectroscopic Coronagraph (LASCO). Sol. Phys. 162, 357–402, 1995.

Cranmer, S.R., Kohl, J.L., Noci, G., et al. An Empirical Model of a Polar Coronal Hole at Solar Minimum. ApJ 511, 481–501, 1999.

Dulk, G.A., Jacques, S., Smerd, S.F., et al. White light and radio studies of the coronal transient of 14-15 September 1973. I - Material motions and magnetic field. Sol. Phys. 49, 369–394, 1976.

Gibson, S.E., Fludra, A., Bagenal, F. Solar minimum streamer densities and temperatures using Whole Sun Month coordinated data sets. JGR 104, 9691–9700, 1999.

Gopalswamy, N., Yashiro, S., Michalek, G., et al. The SOHO/LASCO CME Catalog. Earth, Moon, and Planets 104, 295–313, 2009.

Ingleby, L.D., Spangler, S.R., Whiting, C.A. Probing the Large-Scale Plasma Structure of the Solar Corona with Faraday Rotation Measurements. ApJ 668, 520–532, 2007.

Kohl, J.L., Esser, R., Gardner, L.D., et al. The Ultraviolet Coronagraph Spectrometer for the Solar and Heliospheric Observatory. Sol. Phys. 162, 313–356, 1995.

Korreck, K.E., Zurbuchen, T.H., Lepri, S.T., Raines, J.M. Heating of Heavy Ions by Interplanetary Coronal Mass Ejection Driven Collisionless Shocks. ApJ 659, 773–779, 2007.

Mancuso, S., Spangler, S.R. Faraday Rotation and Models for the Plasma Structure of the Solar Corona. ApJ 539, 480–491, 2000.

Mancuso, S., Raymond, J.C., Kohl, J., et al. UVCS/SOHO observations of a CME-driven shock: Consequences on ion heating mechanisms behind a coronal shock. Astron. Astrophys. 383, 267–274, 2002.

Mancuso, S., Raymond, J.C., Kohl, J., et al. Plasma properties above coronal active regions inferred from SOHO/UVCS and radio spectrograph observations. Astron. Astrophys. 400, 347–353, 2003.

Mancuso, S., Avetta, D. UV and Radio Observations of the Coronal Shock Associated with the 2002 July 23 Coronal Mass Ejection Event. ApJ 677, 683–691, 2008.

Ontiveros, V., Vourlidas, A. Quantitative Measurements of Coronal Mass Ejection-Driven Shocks from LASCO Observations. ApJ 693, 267–275, 2009.

Pagano, P., Raymond, J.C., Reale, F., Orlando, S. Modeling magnetohydrodynamics and non-equilibrium SoHO/UVCS line emission of CME shocks. Astron. Astrophys. 481, 835–844, 2008.

Patzold, M., Bird, M.K., Volland, H., et al. The mean coronal magnetic field determined from HELIOS Faraday rotation measurements. Sol. Phys. 109, 91–105, 1987.

Priest, E.R. Solar Magnetohydrodynamics. Reidel Pub. Co., Dordrecht, Holland, 1982.

Raymond, J.C., Thompson, B.J., St. Cyr, O.C., et al. SOHO and radio observations of a CME shock wave. Geophys. Res. Lett. 27, 1439–1442, 2000.

Smerd, S.F., Sheridan, K.V., Stewart, R.T. On Split-Band Structure in Type II Radio Bursts from the Sun. IAU Symp. no. 57, 389-393, 1974.

Van de Hulst, H.C. The electron density of the solar corona. Bull. Astron. Inst. Netherlands 11, 135–149, 1950.

Vourlidas, A., Wu, S.T., Wang, A.H., Subramanian, P., Howard, R.A. Direct Detection of a Coronal Mass Ejection-Associated Shock in Large Angle and Spectrometric Coronagraph Experiment White-Light Images. Astrophys. J. 598, 1392–1402, 2003.

Vourlidas A. Detections of CME-Driven Shocks with LASCO. SOHO-17. 10 Years of SOHO and Beyond, ESA SP-617, 2006.

Vršnak, B., Aurass, H., Magdalenic, J., Gopalswamy, N. Band-splitting of coronal and interplanetary type II bursts. I. Basic properties. Astron. Astrophys. 377, 321–329, 2001.

Vršnak, Magdalenic, J., Aurass, H., Mann, G. Band-splitting of coronal and interplanetary type II bursts. II. Coronal magnetic field and Alfvén velocity. Astron. Astrophys. 396, 673–682, 2002.